Supplementary Methods

Animal preparation. Cats (postnatal day 28-35) were prepared for intrinsic-signal and two-photon calcium imaging. Anaesthesia was induced with ketamine (20 mg kg^{-1}, intramuscularly) and acepromazine (0.2 mg kg^{-1}, intramuscularly), and continued with isoflurane (1-2 % in surgery, 0.5-1% during imaging). The animals were paralysed with vecuronium bromide (0.2-0.4 mg kg^{-1} hr^{-1}, intravenously) and expired CO_2 regulated at 3.5-4.5% via mechanical ventilation. After fixing the skull with a head plate, a small craniotomy was carried out over the visual cortex, the dura reflected and the underlying cortex covered with agarose (3% in artificial cerebrospinal fluid, ACSF). All surgical and experimental procedures were in accordance with National Institutes of Health and United States Department of Agriculture guidelines and were approved by the Harvard Medical Area Standing Committee on Animals.

Intrinsic-signal optical imaging. The cortex was illuminated with 630 nm light and the camera was focused 400 µm below the cortical surface. Images were obtained with a CCD video camera (748 x 480 pixels) and digitised by Imager 3001 (Optical Imaging, Mountainside, NJ). To obtain single-condition maps, the images for each stimulus were divided by a 'cocktail blank', the sum of the images for all stimuli. Then the single-condition maps were spatially smoothed (Gaussian, σ = 50 µm) and the preferred orientation for each pixel was obtained by vector summation (see Fig. 1a). Using the surface blood vessel pattern, we targeted a pinwheel centre with a glass pipette to inject the cell-permeant calcium indicator. For several reasons, the injection site was not always exactly at the pinwheel center. The penetration angle of the pipette was very oblique (~ 30 degrees relative to the cortical surface) and the need to avoid surface blood vessels made exact targeting of the pipette difficult. As a result, the pipette tip was often located 50-100 µm away from the pinwheel center.

Two-photon calcium imaging *in vivo*. A total of 0.8 mM Oregon Green 488 BAPTA-1 AM (OGB-1 AM) was dissolved in DMSO with 20% pluronic acid and diluted 1:10 in ACSF containing 40 μM Alexa-594 (all from Molecular Probes). A patch pipette (tip diameter: 2-3 μm) was filled with this solution and inserted into the cortex to a depth of 200–250 μm from the surface. OGB-1 AM and Alexa-594 were pressure ejected from the pipette (5-10 psi for 30-60 s). Two-photon imaging of changes in calcium fluorescence in cortical neurons was monitored with a Leica TCS SP2 microscope coupled with a Mira 900 (Coherent Systems) mode-locked Ti:sapphire laser (810 nm). Excitation light was focused by a 40X (NA 0.8) or 20X (NA 0.5) water immersion objective. A square region of 300 (with 40X) or 600 μm (with 20X) side length was imaged at 512 x 512 pixels at 1.63 s per frame. The average power delivered to the brain was < 45 mW for 300 μm of image size and < 80 mW for 600 μm. In all experiments, images were obtained from multiple depths spaced by 10 or 20 μm.

Visual stimulation. Square-wave gratings at 100% contrast (red bars on a black background, which mostly did not pass the green filter we used for calcium imaging) were drifted at 2 Hz on a 15-inch LCD monitor at eight or sixteen directions of motion in 22.5° or 45° steps. Spatial frequency was 0.05-0.15 cycles per degree. Each stimulus started with a blank period of uniform luminance (8 s) followed by the same period of visual stimulation. The eight or sixteen stimuli were presented sequentially and repeated ten times. In most cases, the animals were stimulated binocularly. In some experiments, we also stimulated the contralateral or ipsilateral eye alone and obtained essentially the same results.

Data Analysis. Two-photon images were analysed in Matlab (Mathworks) and ImageJ (National Institutes of Health). Time-lapse images were realigned by maximizing the correlation between frames, to remove slow tangential drift (< several μm) of the brain over >10 minutes of scanning time. Cells were automatically identified (6,616 cells in 10

pinwheels) through a series of morphological filters that delineated the contours of cell bodies based on intensity, size, and shape. Cell outlines were visually inspected and the rare but clear errors were corrected manually. The position of each cell was obtained as the centre of gravity of the soma. Fluorescence time courses of individual cells were extracted by summing pixel values within cell contours. Slow drift of the baseline signal over minutes was removed by a low-cut filter (cut-off: 4 minutes). Visually responsive cells were defined by ANOVA across the blank and eight directions ($p < 0.05$; 6,126 cells, 92.6%). Of these, selective cells were defined by ANOVA across eight directions ($p < 0.05$; 6,026 cells, 91.1%). In cell maps (Fig. 1c-e, 2a, 3a), only selective cells are colour-coded. Preferred orientation was obtained by vector averaging. Tuning curves (Fig. 2b-e) were fit with the sum of two circular Gaussian functions (von Mises distribution: $A \exp(-k (1-\cos(\varphi - \varphi_0))))$[1]. Preferred direction was defined as the peak of this best-fit curve. In some experiments, the cortical surface was tilted from the imaging plane. The tilt angle was estimated from the layer 1/2 border or the cortical surface. To align the images from multiple depths, the tilt was corrected by shifting images (see grey margins in Fig. 1c). The exact position of the pinwheel centre was determined from the aligned image stack by minimizing the *angular deviation* (deviation of preferred orientation of individual cells from azimuth-orientation function in Fig. 3b) of all cells within the central 65 µm (see Fig. 3a-e).

1. Swindale, N. V., Grinvald, A., Shmuel, A. The spatial pattern of response magnitude and selectivity for orientation and direction in cat visual cortex. *Cereb. Cortex* 13, 225-38 (2003).

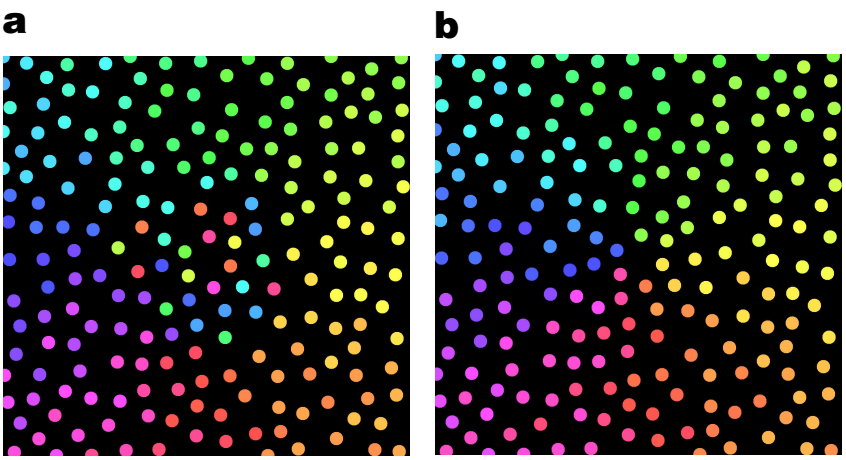

Supplementary Figure 1 Two possible arrangements of neurons at a pinwheel centre, which are consistent with previous imaging and electrophysiological studies. Each colour represents the preferred orientation of individual neurons. **a**, neurons selective for different orientations are arranged randomly near the pinwheel centre. **b**, neurons are perfectly segregated up to the very centre according to their preferred orientations. In either case, neurons preferring different orientations would be recorded simultaneously, if an electrode was targeted to the pinwheel centre.[1]

1. Maldonado, P. E., Godecke, I., Gray, C. M. & Bonhoeffer, T. Orientation selectivity in pinwheel centers in cat striate cortex. *Science* **276**, 1551-1555 (1997).

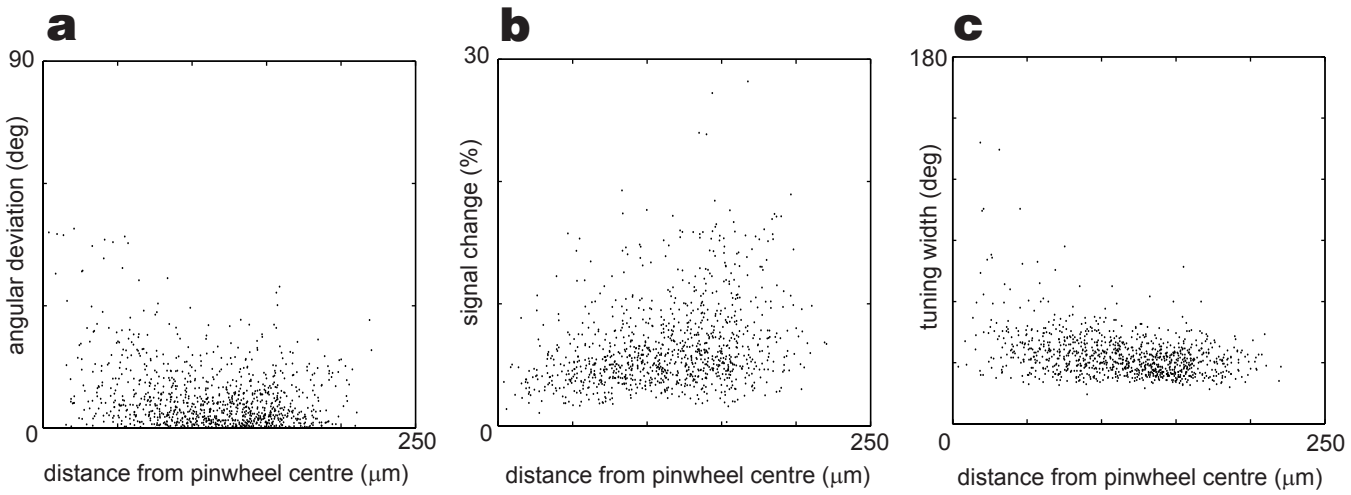

Supplementary Figure S2 Dependence of properties of individual neurons as a function of distance from the pinwheel centre. **a**, angular deviation of preferred orientation (see text for definition), **b**, fluorescence signal change to optimal orientation, **c**, tuning width (half width at half maximum). Each dot represents one cell, and all data from nine depths of one pinwheel (Fig. **1c**) are shown.

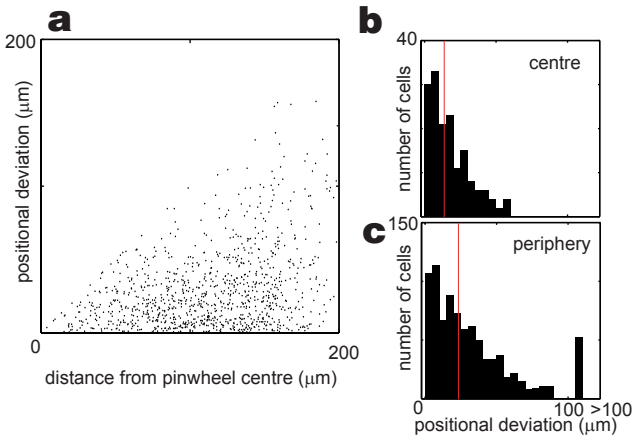

Supplementary Figure S3 *Positional deviation*. The degree to which individual cells deviated from the orderly pinwheel arrangement is quantified as positional error. In Figure **3c-e**, the deviation is quantified as *angular deviation*, which indicates how many degrees the preferred orientation of each cell deviates from the *azimuth-orientation function* (black curve in Figure **3b**). The *positional deviation* was obtained as the shortest distance between each cell and the *iso-orientation domain* of the same preferred orientation, derived from the *azimuth-orientation function*. **a**, *positional deviation* is plotted against distance from the pinwheel centre. Note that the *positional deviation* is even smaller at the pinwheel centre than in the periphery. **b**, **c**, Histograms of *positional deviation* for all the selective cells near the pinwheel centre (**b**) and in the periphery (**c**). Median value of distribution is significantly smaller at the centre (indicated by the red lines; 14 μm for centre, and 24 μm for periphery; $p < 10^{-6}$; Wilcoxon rank-sum test).

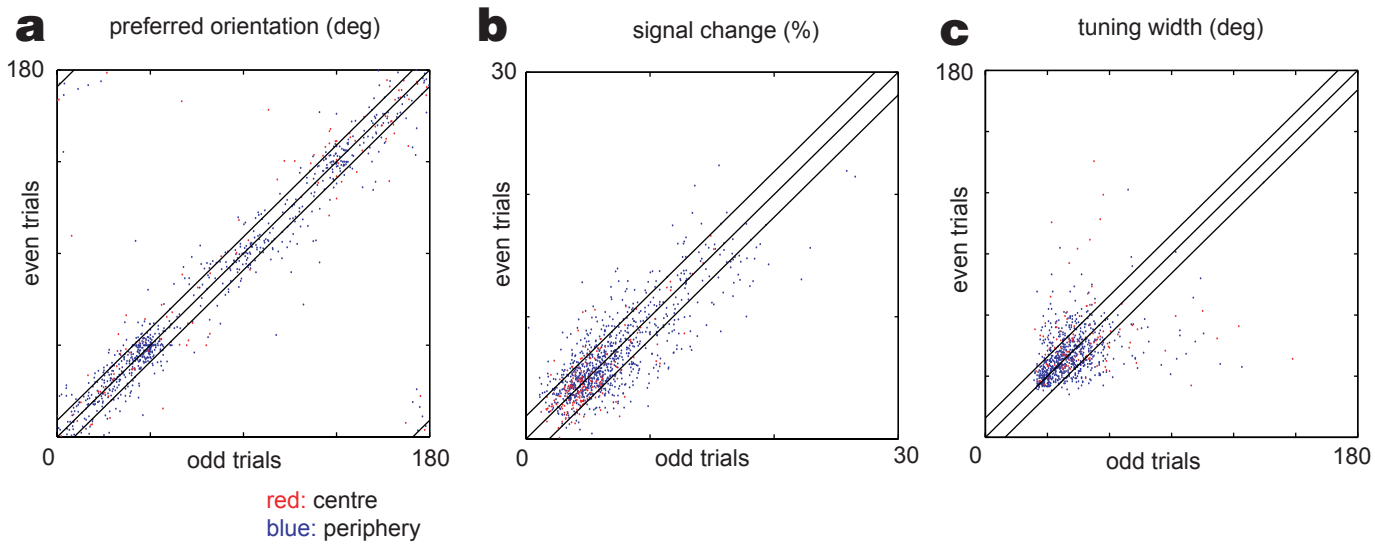

Supplementary Figure S4 Reproducibility of tuning properties of single cells. A total of ten trials was separated into the odd five trials and the even five trials. Then, the tuning properties of individual neurons were calculated from the averages of these odd and even trials, respectively. **a**, preferred orientation, **b**, signal change to optimal orientation, and **c**, tuning width (half width at half maximum). In each panel, values obtained from the odd trials was plotted against values from the even trials. Red points represent neurons at the pinwheel centre, and blue points represent neurons in the periphery. The estimation was accurate for preferred orientation (**a**) and response strength (**b**): the standard deviation of the difference (see diagonal lines) was 8 degrees for preferred orientation and 1.9% for response strength. The estimation was less accurate for tuning width (**c**), for which the standard deviation was 10 degrees.

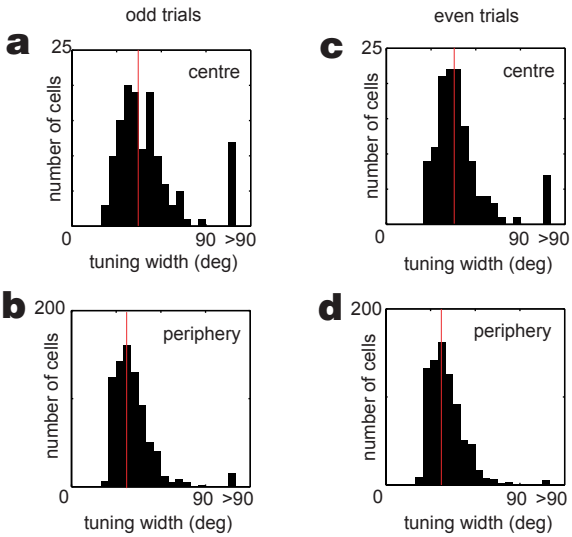

Supplementary Figure S5 Reproducibility of the distribution of tuning widths in a population of neurons. The distributions of the tuning widths in a population of neurons were obtained from odd trials (**a**, **b**) and even trials (**c**, **d**), separately. The histograms are similar for odd and even trials; in particular, the difference between centre and periphery is consistent ($p < 0.0001$ for both odd and even trials; Wilcoxon rank-sum test). Thus, the distribution of the tuning widths in a population of neurons is robust, although the estimation of the tuning widths of individual neurons is less accurate (see Supplementary Fig. S3c).

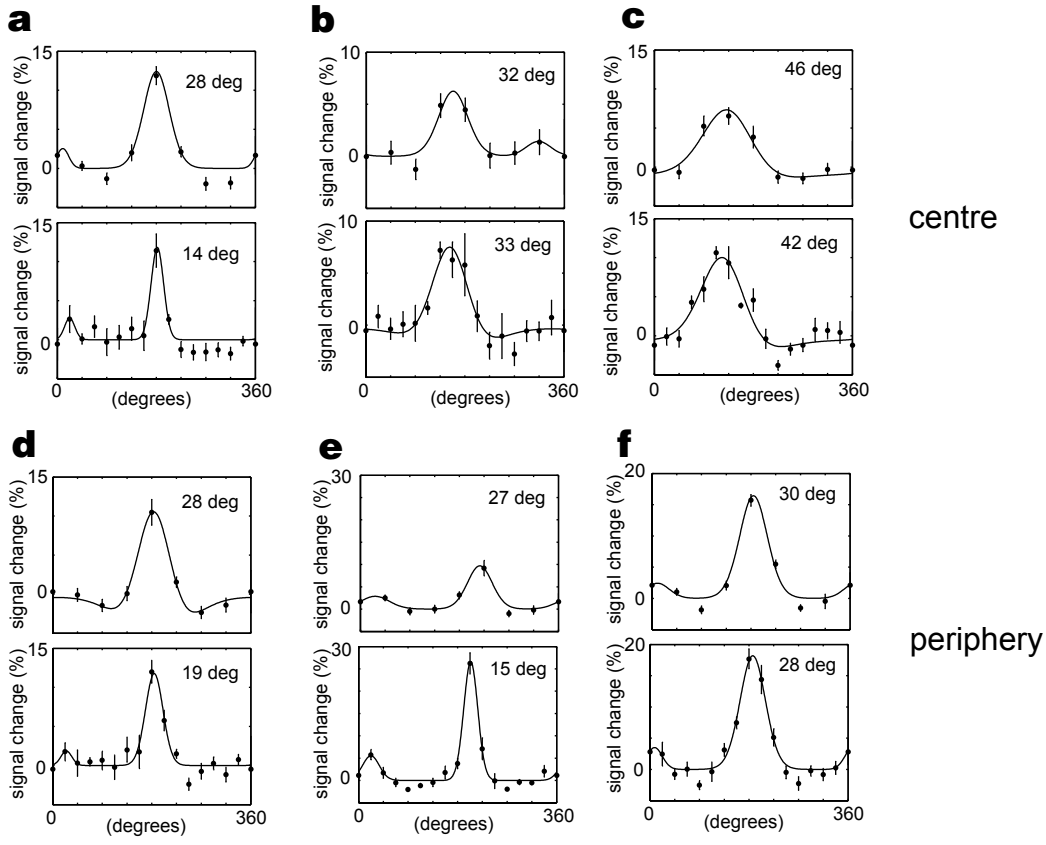

Supplementary Figure S6 Tuning curves of six neurons measured with intervals of 45 degrees (upper in each panel) and 22.5 degrees (lower). **a-c**, three cells in the pinwheel centre, **d-f**, three cells at the periphery. Error bars: standard error of mean (n=10 for 45 degrees, and n=5 for 22.5 degrees). The tuning width obtained from curve fitting (see Methods) is displayed at the top-right corner of each panel. In very sharply tuned cells (**a**, **d**, **e**), the tuning width obtained with 22.5 degrees tends to be less than that obtained with 45 degrees intervals. Such sharply tuned cells are often found in the periphery (**d**, **e**), and less often in the centre (**a**). In cell **e**, the best orientation (200.5 degrees) is not sampled with 45 degrees intervals, which is why the tuning amplitude appears smaller in the upper panel. In relatively broadly tuned cells (**b**, **c**, **f**), the tuning widths do not strongly depend on the sampling intervals.

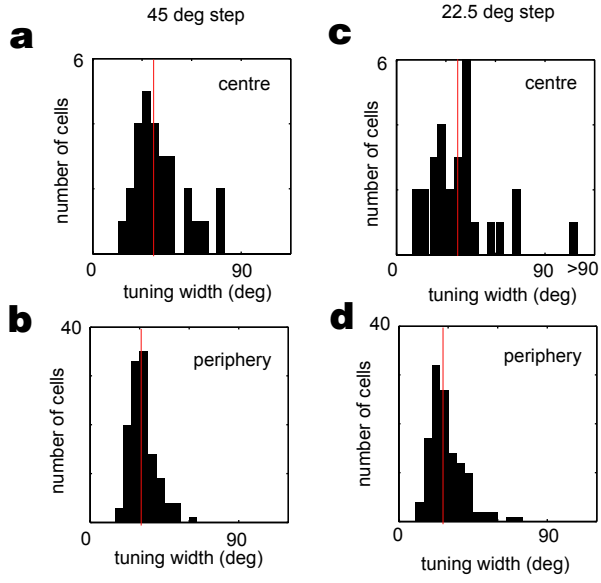

Supplementary Figure S7 Histograms of tuning width measured with intervals of 45 degrees (**a**, **b**) and 22.5 degrees (**c**, **d**), for pinwheel centre (**a**, **c**), and periphery neurons (**b**, **d**). As demonstrated in Supplementary Fig. **S6**, finer sampling (22.5 degrees) tends to give smaller tuning widths for very sharply tuned cells. This tendency was found in the periphery (**b**, **d**; median value: 31 degrees for 45 degree intervals, 27 degrees for 22.5 degree intervals) in this specific experiment, and also in the other two experiments in which the orientation was sampled both at 45 and 22.5 degree intervals. Near the pinwheel centre, sharply tuned cells were less often found, and the median value of the distribution did not depend on the sampling interval (**a**, **c**; 38 degrees for both). A significant difference between centre and periphery was consistently found with both 22.5 and 45 degree sampling intervals ($p < 0.01$; Wilcoxon rank-sum test), but finer sampling enlarged the apparent magnitude of this difference.

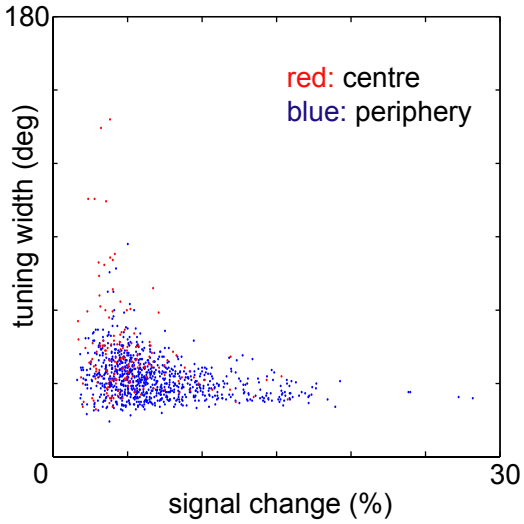

Supplementary Figure S8 Scatter plot of response magnitude (ΔF/F) versus orientation tuning width. Red and blue dots represent cells in the centre (< 65 μm) or periphery (> 65 μm), respectively, of the pinwheel shown in Fig. 1c. The tuning width was inversely correlated with response strength both near the centre and in the periphery ($p < 0.0001$). All of the cells with the broadest tuning width (> 70 degrees; see the right tails of the histograms in Fig. 3i, j) showed less than 5.1% signal change, which was close to the noise level.

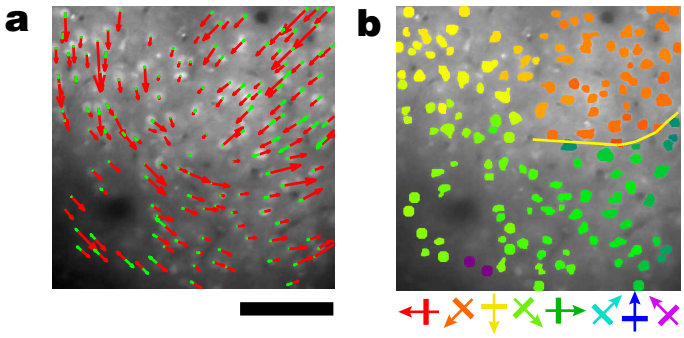

Supplementary Figure S9 Maps of a direction fracture terminating in a pinwheel centre. **a**, Vector map of preferred direction of all tuned cells. Red and green arrows indicate the response magnitudes at the preferred and null directions, respectively. Scale bar, 100 μm. **b**, Colour-coded direction map, according to the colour key below. Around this specific pinwheel, only directions between 45 degrees and 225 degrees were observed (from orange to blue-green), although two cells in the bottom left show a direction preference near 315 degrees. The direction fracture (yellow line) can be seen as the border between cells labelled orange and blue-green.

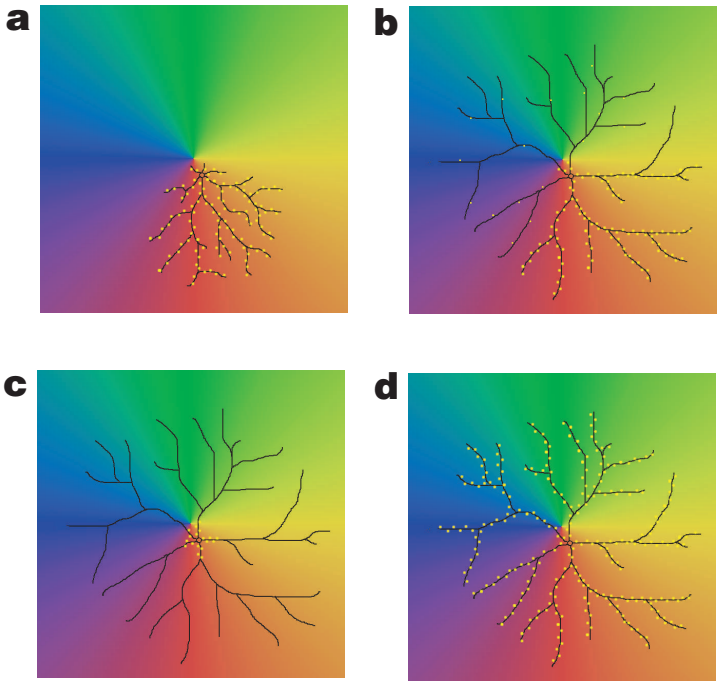

Supplementary Figure S10 Potential scenarios ensuring sharp orientation tuning of neurons near pinwheel centres. The background colour represents the preferred orientation of afferent inputs, *i.e.* the local axons, which are assumed to be well segregated. The dendritic arbour of a neuron with a somata located a few tens of micrometres away from the pinwheel centre is depicted, with yellow dots indicating excitatory synapses. In the model illustrated in panel **a**, the overall morphology of the dendritic arbour is biased towards one iso-orientation domain, thus providing the cell with sharply tuned inputs. In the models illustrated in **b-d**, the dendritic arbour is assumed to be symmetric. In **b**, the dominant excitatory inputs are biased towards the iso-orientation domain, although the overall dendritic morphology is symmetric. In **c**, the dominant inputs are symmetric, but they are proximal to the cell body. Because the cell body is slightly displaced from the centre of the pinwheel, these inputs will be sharply tuned if afferent inputs are well segregated near the pinwheel centre. In **d,** synaptic inputs are integrated uniformly throughout the dendritic arbour, including regions tuned to different orientations. This would lead to only a slight bias in the orientation tuning of the inputs, which could be sharpened by output nonlinearity, such as the spike threshold. It is assumed that one side of each panel is 600 μm, and the radius of the dendritic arbour is approximately 250 μm.